

1 Activation of sodium persulfate by magnetic carbon xerogels (CX/CoFe) for the oxidation of
2 bisphenol A: Process variables effects, matrix effects and reaction pathways

3
4 Alexandra Outsiou^a, Zacharias Frontistis^a, Rui S. Ribeiro^{b,c}, Maria Antonopoulou^d, Ioannis K.
5 Konstantinou^e, Adrián M.T. Silva^c, Joaquim L. Faria^c, Helder T. Gomes^b, Dionissios
6 Mantzavinos^{a*}

7
8 ^a *Department of Chemical Engineering, University of Patras, Caratheodory 1, University*
9 *Campus, GR-26504 Patras, Greece.*

10 ^b *Laboratory of Separation and Reaction Engineering - Laboratory of Catalysis and Materials*
11 *(LSRE-LCM), Escola Superior de Tecnologia e Gestão, Instituto Politécnico de Bragança,*
12 *Campus de Santa Apolónia, 5300-253 Bragança, Portugal.*

13 ^c *Laboratory of Separation and Reaction Engineering – Laboratory of Catalysis and*
14 *Materials (LSRE-LCM), Faculdade de Engenharia, Universidade do Porto, Rua Dr. Roberto*
15 *Frias, 4200-465 Porto, Portugal.*

16 ^d *Department of Environmental and Natural Resources Management, University of Patras, 2*
17 *Seferi St., GR-30100 Agrinio, Greece.*

18 ^e *Department of Chemistry, Laboratory of Industrial Chemistry, University of Ioannina, GR-*
19 *45110 Ioannina, Greece.*

20 *Corresponding author

21 E-mail: mantzavinos@chemeng.upatras.gr; Tel.: +302610996136; Fax: +302610969532

22

23

24 This article has been accepted for publication and undergone full peer review.
25 Please cite this article as DOI: 10.1016/j.watres.2017.07.046

26

27 Abstract

28 An advanced oxidation process comprising sodium persulfate (SPS) and a novel magnetic
29 carbon xerogel was tested for the degradation of bisphenol A (BPA), a model endocrine-
30 disrupting compound. The catalyst, consisting of interconnected carbon microspheres with
31 embedded iron and cobalt microparticles, was capable of activating persulfate to form sulfate
32 and hydroxyl radicals at ambient conditions.

33 The pseudo-first order degradation rate of BPA in ultrapure water (UPW) was found to
34 increase with (i) increasing catalyst (25-75 mg/L) and SPS (31-250 mg/L) concentrations, (ii)
35 decreasing BPA concentration (285-14200 µg/L), and (iii) changing pH from alkaline to
36 acidic values (9 to 3).

37 Besides UPW, tests were conducted in drinking water, treated wastewater, groundwater and
38 surface water; interestingly, the rate in UPW was always lower than in any other matrix
39 containing several organic and inorganic constituents. The effect of natural organic matter (in
40 the form of humic acids) and alcohols was detrimental to BPA degradation owing to the
41 scavenging of radicals. Conversely, chlorides at concentrations greater than 50 mg/L had a
42 positive effect due to the formation and subsequent participation of chlorine-containing
43 radicals.

44 Liquid chromatography time-of-flight mass spectrometry was employed to identify major
45 transformation by-products (TBPs) of BPA degradation in the absence and presence of
46 chlorides; in the latter case, several chlorinated TBPs were detected confirming the role of Cl-
47 related radicals. Based on TBPs, main reaction pathways are proposed.

48 *Keywords:* chloride; endocrine disruptors; Fenton-like; intermediates; operating parameters;
49 radicals.

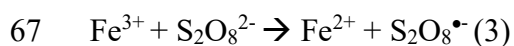
50

51 1. Introduction

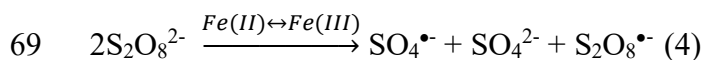
52 In recent years, the use of persulfate as a source of reactive sulfate radicals (equation 1) has
53 been considered an efficient advanced oxidation process (AOP) for water and wastewater
54 treatment (Matzek and Carter, 2016):



56 Persulfate exhibits several advantages due to its moderate cost, high stability and aqueous
57 solubility, as well as to the fact that it is solid at ambient temperature, which facilitates its
58 transport and storage (Lin et al., 2011). Nonetheless, persulfate itself is a moderate oxidizing
59 agent ($E^\circ=2.01$ V) and it must be activated to generate sulfate radicals ($E^\circ=2.5-3.1$ V), which
60 typically react 103-105 times faster than the anion persulfate (Tsitonaki et al., 2010).
61 Persulfate activation can be achieved by several means including heat, UV light, ultrasound,
62 microwaves and through one-electron transfer using metals such as iron, cobalt, copper, zinc
63 and manganese (Matzek and Carter, 2016). Persulfate activation by transition metals and,
64 ferrous ion in particular, has extensively been investigated mimicking classical Fenton
65 reactions (Liu et al., 2014) (equations 2-4):



68 Thus, the overall metal-catalyzed decomposition of persulfate can be described as follows:



70 In Fenton and alike systems, the use of homogeneous iron (or other ions) typically requires an
71 additional step for the recovery and/or elimination of metals from the treated stream prior to
72 final discharge. Several attempts have been made to overcome this drawback through
73 immobilization of the active phase on a suitable support, i.e. activated carbon, alumina, silica,
74 mesoporous molecular sieves, zeolites, pillared clays and ion-exchange resins (Nidheesh,

75 2015). Nevertheless, this approach may result in reduced efficiency associated with decreased
76 catalyst stability and/or increased mass transfer limitations (Ribeiro et al., 2016a).

77 A set of novel magnetic carbon xerogels, consisting of interconnected carbon microspheres
78 with iron and/or cobalt microparticles embedded in their structure, has recently been prepared
79 by inclusion of iron and/or cobalt precursors during the synthesis of carbon xerogels by
80 polycondensation of resorcinol with formaldehyde, followed by thermal annealing at 800°C.

81 The catalysts have extensively been characterized and tested successfully for the oxidation of
82 the antibiotic sulfamethoxazole in water using hydrogen peroxide as the source of hydroxyl
83 radicals; these materials exhibited high activity and good stability and they were also
84 magnetically recoverable post-treatment (Ribeiro et al., 2016b).

85 The work reported in this paper deals for the first time with the use of magnetic carbon
86 xerogels as possible activators of persulfate to oxidize bisphenol A (BPA) in various aqueous
87 matrices. BPA is an emerging micro-contaminant belonging to the family of endocrine
88 disruptors and it has been chosen as a model compound due its excessive usage in plastics
89 manufacturing, as well as additive in brake fluids, thermal papers and flame retardants
90 (Oehlmann et al., 2008). BPA exhibits weak estrogenic activity at concentrations as low as
91 few ng/L-µg/L, while it is resistant to biodegradation (Vandenberg et al., 2007). It can be
92 released in the environment through various paths including municipal wastewater treatment
93 plant discharges, landfill leachates and spillovers during storage/transportation (Huang et al.,
94 2012).

95 The goal of this work was to study the effect of various operating parameters such as the
96 concentration of catalyst, the concentration of persulfate, the concentration of BPA and the
97 solution pH on the kinetics of degradation. Particular emphasis was given on the effect of the
98 matrix complexity testing several environmentally relevant water matrices. In addition, major
99 transformation by-products were identified and possible reaction pathways and mechanisms
100 were proposed, taking into consideration the interferences of the water matrix constituents.

101

102 2. Materials and methods

103 2.1 *Magnetic carbon xerogels*

104 Experiments were performed with a bimetallic carbon xerogel consisting of interconnected
105 carbon microspheres with iron and cobalt microparticles embedded in their structure
106 (CX/CoFe). Cobalt ferrite (CoFe_2O_4) is the dominant phase. The procedures for catalyst
107 synthesis and characterization are described in detail elsewhere (Ribeiro et al., 2016b).

108

109 2.2 *Chemicals*

110 Bisphenol A (BPA, $\text{C}_{15}\text{H}_{16}\text{O}_2$, CAS number: 80-05-7) and sodium persulfate (SPS, $\text{Na}_2\text{S}_2\text{O}_8$,
111 99+%, CAS number: 7775-27-1) were purchased from Merck.

112 Humic acid (technical grade), hydrogen peroxide (30%), sodium chloride (99.8%), sodium
113 hydroxide (98%), boric acid (>99.8%) and sulphuric acid (95%) were also obtained from
114 Merck. Methanol (99.9%) and t-butanol (99%) were purchased from Fluka, while potassium
115 dihydrogen phosphate from Millipore.

116 All chemicals were used as received, without further purification.

117

118 2.3 *Water matrices*

119 BPA solutions were prepared in (i) ultrapure water (UPW); (ii) secondary treated wastewater
120 (WW) collected from the wastewater treatment plant of the University of Patras campus,
121 Greece; (iii) drinking water (DW) obtained from a bottle of the commercially available brand
122 Avra®, Greece; (iv) surface water taken from a rivulet in the region of Athens, Greece; (v)
123 groundwater taken from a borehole in the region of Athens, Greece. Properties of the various
124 matrices are summarized in Table 1.

125

126 *2.4 Experimental procedure*

127 In a typical experiment, 120 mL of an aqueous solution containing the desired concentration
128 of BPA was loaded in a glass cylindrical reaction vessel. The appropriate amount of SPS and
129 the catalyst were then added and the reaction took place under magnetic stirring in open air
130 equilibrium. Unless otherwise stated, the solution was buffered at acidic, near-neutral or
131 alkaline conditions using the appropriate buffers (see section 3.1). Samples of 1.2 mL were
132 periodically withdrawn from the reactor, quenched with methanol, filtered to remove any
133 solid particles and analyzed by chromatography.

134 Most of the experiments were performed in duplicate and mean values (<5% difference) are
135 quoted as results.

136

137 *2.5 Analytical methods*

138 High performance liquid chromatography was employed to monitor the concentration of
139 BPA. The analytical protocol (columns, mobile phase, detector) is described in detail
140 elsewhere (Darsinou et al., 2015). The limit of detection was 4.7 µg/L and the limit of
141 quantitation was 12.4 µg/L.

142 Liquid chromatography time-of-flight mass spectrometry (LC-TOF-MS) operated in negative
143 ionization mode was used for the identification of transformation by-products (TBPs) as
144 described in detail in our previous work (Darsinou et al., 2015). LC analyses were run with
145 water (LC-MS grade) with 0.01% formic acid (solvent A) and acetonitrile (solvent B) as
146 mobile phase with a flow rate of 0.3 mL/min. A linear gradient was run as follows: 1% B
147 (initial conditions) to 99% B in 15 min and then returned to 1% B after 3 min.

148

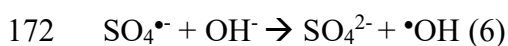
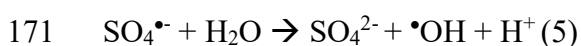
149 **3. Results and discussion**

150 *3.1 Effect of solution pH*

151 The effect of solution pH on BPA degradation was studied at three values, i.e. 3, 6 and 9. The
152 results are shown in Figure 1. Near-neutral and alkaline conditions were achieved using
153 KH_2PO_4 and a mixture of NaOH and H_3BO_3 as buffers, respectively, while acidic conditions
154 were achieved adding H_2SO_4 , which also served as buffer; in all cases, the pH remained
155 unchanged during the reaction. Although complete BPA degradation can be achieved within
156 45-60 min regardless of the starting solution pH, the initial rate decreases with increasing pH.
157 The point of zero charge of the catalyst is 7.7 (Ribeiro et al., 2016b), therefore, it is positively
158 charged at $\text{pH} < 7.7$. Consequently, the adsorption and subsequent activation of persulfate
159 anions onto the catalysts is favored at pH values of 3 and 6 due to the electrostatic attraction
160 between the catalyst surface and the persulfate ions but it decreases at $\text{pH} = 9$ due to
161 electrostatic repulsion. In addition, the presence of insoluble forms of Fe(II)/Fe(III) under
162 neutral and alkaline pH could be also considered for the slower kinetics obtained at pH 6 and
163 9.

164 Furthermore, BPA whose pK_a is 9.6-10.2 (Bautista-Toledo et al., 2005), is negatively charged
165 at alkaline pH range above the pK_a value, therefore, an electrostatic repulsion between the
166 substrate and the catalyst cannot be considered to affect significantly the degradation kinetics
167 and thus the decreased reactivity recorded at $\text{pH} = 9$.

168 Finally, sulfate radicals react with water at all pH values leading to the formation of hydroxyl
169 radicals, which become the main oxidizing species at alkaline conditions (Matzek and Carter,
170 2016; Zhao et al., 2014), according to equations 5 and 6:



173 Although sulfate radicals have a lower redox potential than hydroxyl radicals, they are more
174 selective towards certain organics (Darsinou et al., 2015; Lutze et al., 2015) and this may
175 justify the reactivity recorded at lower pH values, where sulfate radicals prevail.

176 Additional experiments (not shown for brevity) were performed adjusting but not buffering
177 the initial solution pH from its inherent value of 6 to 9 (with NaOH) or 3 (with H₂SO₄). For
178 the run at pH₀=6, the value rapidly dropped to 4.3 within the first 2 min of reaction and
179 eventually stabilized to 4±0.2 for the rest of the reaction; at these conditions, the BPA
180 degradation profile nearly matched that at pH₀=3. For the run at pH₀=9, the degradation was
181 always 15-20% lower than at the other two pHs, with pH dropping and stabilizing at near-
182 neutral values.

183 These results indicate that the proposed treatment system can function efficiently in a wide
184 range of pH values, which makes its application feasible for water/wastewater treatment
185 without the need for pH buffering or adjustment (i.e. at the sample's natural pH). However
186 and for the purposes of this study, all subsequent experiments were performed at pH=3 in
187 order to eliminate the effect of pH change during the reaction.

188

189 *3.2 Effect of catalyst and SPS concentration*

190 Based on the knowledge for Fenton and Fenton-like reactions in which the concentration
191 levels of the catalyst and the oxidant are crucial to process performance, the effect of these
192 parameters are also studied herein. Figure 2 shows the beneficial effect of increasing catalyst
193 concentration in the range 25-75 mg/L on the degradation of 285 µg/L BPA. Considering that
194 BPA concentration-time profiles can be fitted adequately (i.e. the linear regression coefficient,
195 r^2 , is >95%) to a pseudo-first order rate expression (equation 7):

$$196 \quad \ln \frac{C_o}{C} = k_{app}t \Leftrightarrow \ln(1 - X) = -k_{app}t \quad (7)$$

197 the apparent rate constant for BPA degradation, k_{app} , is computed equal to 0.013, 0.038 and
198 0.094 min⁻¹ at 25, 50 and 75 mg/L catalyst concentration, respectively. In the absence of
199 catalyst, SPS cannot be activated to form radicals and this is consistent with the low extent

200 (*ca* 10%) of BPA degradation recorded (this is due to the fact that SPS itself is a mild
201 oxidant).

202 Figure 3 shows the effect of changing SPS concentration in the range 31-500 mg/L on the
203 degradation of 285 µg/L BPA. The computed k_{app} values according to equation 7 are 0.054,
204 0.069, 0.086, 0.093 and 0.046 min⁻¹ at 31, 62.5, 125, 250 and 500 mg/L SPS, respectively (the
205 linear regression coefficient, r^2 , is >97%). Degradation increases with increasing SPS
206 concentration up to a point, beyond which the effect becomes detrimental; it is well-
207 documented (Dewil et al., 2017) that an excess of oxidant in Fenton and alike systems may
208 result in radical self-scavenging effects, thus decreasing performance. From the experiment
209 without SPS, it is evident that BPA is partly adsorbed onto the catalyst surface (i.e. 30% after
210 45 min, which is extended to 35% after 90 min (not shown in Figure 3)).

211 We have recently demonstrated (Ribeiro et al., 2016b) that carbon xerogels are effective
212 heterogeneous Fenton catalysts for the degradation of antibiotics in various matrices. In this
213 light, an additional experiment was performed replacing SPS with an equal concentration of
214 H₂O₂; as can be seen in Figure 3, the reaction with 250 mg/L H₂O₂ is substantially slower
215 leading to only 63% BPA degradation after 45 min.

216

217 *3.3 Effect of BPA concentration*

218 Although the pseudo-first order approach is useful to depict apparent rate constants and,
219 consequently, quantify kinetics, this does not necessarily imply that the reaction is indeed true
220 first order with respect to the substrate. This is clearly demonstrated in Figure 4 where the
221 time needed to achieve a certain BPA conversion, X (see also equation 7), depends on its
222 initial concentration. For example, the time needed to achieve 85% BPA conversion is 15, 45
223 and 120 min at 285, 570 and 855 µg/L BPA concentration, respectively; moreover, the
224 corresponding k_{app} are also concentration-dependent taking values of 0.093, 0.042 and 0.019
225 min⁻¹ (r^2 is >94%). As the amount of generated oxidizing species available to react with the

226 substrate mainly depends on the operating conditions (i.e. catalyst and SPS concentration,
227 pH), kinetics will predominantly be dictated by the substrate concentration; as the latter
228 increases, the reaction order will shift to lower values and, eventually, become zero.

229 Although a proper kinetic analysis is outside the scope of this work, the authors would like to
230 emphasize a common misconception made by several researchers in the field concerning the
231 difference between (i) apparent and true rate orders, and (ii) kinetic modeling and data fitting.
232 In several cases, such mistakes are triggered by the unrealistically high contaminant
233 concentrations, e.g. in the order of mg/L, employed in advanced oxidation studies. Figure 4
234 also shows an experiment at 14.2 mg/L BPA concentration leading to just 30% degradation
235 after 120 min. The run was repeated doubling the SPS (500 mg/L) and catalyst (150 mg/L)
236 concentrations and extended to 420 min after which BPA degradation was just 50% (run not
237 shown for brevity).

238

239 *3.4 The water matrix effect*

240 The majority of published research on AOPs for water remediation is being performed in
241 model aqueous solutions containing the contaminant under consideration. Most commonly,
242 the contaminant is spiked in ultrapure water (UPW) at concentrations that typically are
243 several orders of magnitude greater than those found in actual environmental samples (see
244 section 3.3). This approach has certain advantages since (i) it eliminates the interactions
245 amongst the contaminant, the oxidative species and the constituents of more complex
246 matrices (i.e. surface water, groundwater, municipal wastewater), (ii) it does not require
247 sophisticated and laborious analytical techniques to monitor trace amounts of the
248 contaminant.

249 The quality of the actual water matrix is critical since not taking into account the various
250 interactions is likely to lead to false conclusions. As a rule of thumb, degradation kinetics
251 decrease with increasing matrix complexity mainly because the matrix may contain several

252 non-target organic and inorganic constituents that compete with the target molecule(s) for the
253 oxidizing species.

254 Figure 5 shows BPA degradation in various water matrices such as UPW, drinking water
255 (DW), surface water taken from a rivulet, groundwater and secondary treated wastewater
256 (WW). Although complete BPA degradation can be achieved within 30-45 min of reaction
257 irrespective of the matrix employed, the initial rate clearly depends on it. Interestingly, and
258 unlikely to what was expected, the reaction in UPW is slower than in any other matrix
259 including WW, which contains, besides various inorganic anions, organic carbon in the order
260 of 10 mg/L.

261 Humic acids and low molecular weight organic acids such as oxalate are able to form
262 complexes with iron and iron oxides, thus promoting the Fenton-like oxidation processes. On
263 the contrary, the presence of organic matter and inorganic anions could result in competitive
264 adsorption in relation to persulfate anions and substrate onto the xerogel surface, as well as in
265 scavenging of the produced radicals. The observed kinetics is the overall result of interplay
266 among the previous effects and thus we attempted to discriminate the role of the major
267 constituents.

268

269 3.4.1 The role of organic constituents

270 To check the effect of the organic matter, experiments were conducted adding humic acid
271 (HA) in UPW, a representative of the organic matter typically found in natural waters and
272 wastewaters and the results are shown in Figure 6. The apparent rate constant of BPA
273 degradation in UPW is 0.093 min^{-1} and it decreases to 0.058 and 0.036 min^{-1} in the presence
274 of 5 and 20 mg/L HA, respectively. It should be noted here that the organic carbon content of
275 20 mg/L HA is nearly equal to that found in WW. Additional experiments were performed
276 with methanol and t-butanol, which are typical radical scavengers showing different affinity
277 to hydroxyl and sulfate radicals; methanol reacts with the former 300 times faster than with

278 the latter, while t-butanol 1900 times faster (Qi, et al., 2015). The presence of both alcohols
279 retards BPA degradation (the rate constants are 0.031 and 0.023 min⁻¹ with methanol and t-
280 butanol, respectively), indicating that both sulfate and hydroxyl radicals are responsible for
281 BPA degradation. From the results of Figures 5 and 6, it is inferred that the beneficial water
282 matrix effect on BPA degradation cannot be ascribed to the presence of non-target organic
283 constituents as these appear to compete directly with BPA for the oxidizing species. This is
284 also consistent with the effect of initial BPA concentration on its degradation, particularly at
285 excessive concentrations as depicted in Figure 4.

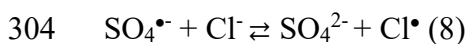
286

287 3.4.2 The role of chloride ion

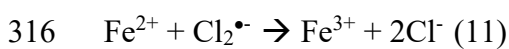
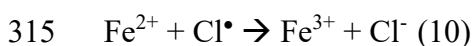
288 Various ions naturally occurring in water matrices may affect the performance of activated
289 persulfate oxidation with bicarbonate and chloride ions playing an important role. The way
290 these ions interfere with the process is case-specific depending on the persulfate activation
291 method, the type of substrate, the complexity of the water matrix and the concentration levels
292 of the ions under consideration; in this respect, it is not surprising that various studies have
293 reported both detrimental and beneficial effects of ions on substrate degradation (Matzek and
294 Carter, 2016; Lutze et al., 2015; Bennedsen et al., 2012; Fang et al., 2012).

295 The effect of chloride in the range 50-500 mg/L on BPA degradation over the CX/CoFe
296 catalyst is shown in Figure 7. The reaction rate increases by as much as six times when the
297 solution is added 200 mg/L chloride, while a higher concentration of 500 mg/L does not
298 accelerate the reaction further. Blank experiments were also performed (not shown for
299 brevity) with NaCl alone (i.e. without catalyst and SPS) and NaCl and SPS (i.e. without
300 catalyst) yielding no BPA degradation.

301 Sulfate radicals primarily react with chloride to form chlorine radicals (equation 8) that
302 further react with chloride to form the dichloride radical (equation 9) (Lutze et al., 2015;
303 Bennedsen et al., 2012; Fang et al., 2012):



306 Depending on the experimental conditions under consideration, several consecutive reactions
307 may take place leading to the formation of additional chlorine-containing radicals such as
308 ClO_2^{\bullet} , ClO^{\bullet} and $\text{HOCl}^{\bullet-}$ (Lutze et al., 2015). From these results, one can safely assume that
309 the presence of chloride influences the distribution and relative concentration of reactive
310 radicals, consequently altering the reactivity towards BPA degradation. Similarly to the
311 present results, the degradation of phenol and 2,4-dichlorophenol by cobalt-activated
312 peroxymonosulfate was promoted in the presence of chloride (Anipstitakis et al., 2006). In
313 addition, chlorine radicals can influence the catalytic step of Fe(II)/Fe(III) conversion, thus
314 regenerating iron in its initial state of Fe(III) in the cobalt ferrite spinel:



317 At acidic conditions ($\text{pH} < 4$), the equilibrium between the bicarbonate ion and CO_2 is
318 completely shifted towards the latter and, in this respect, one might have expected no effect of
319 bicarbonate on the process at the working pH value of 3. Interestingly, experiments with 500
320 mg/L of bicarbonate (data not shown for brevity) resulted in ca 50% reduction of BPA
321 degradation rate (i.e. from 0.093 to 0.045 min^{-1}). As the solution was not purged prior to the
322 experiment to accelerate the release of CO_2 in the atmosphere, the bicarbonate ion may still be
323 present in the solution; its detrimental effect on degradation is associated with the scavenging
324 of both sulfate and hydroxyl radicals to form carbonate radicals (Vicente et al., 2011).

325

326 *3.5. Mechanisms and pathways of degradation*

327 To shed light to the mechanisms of BPA degradation in the presence and absence of chloride,
328 samples were subject to LC-TOF-MS analysis to identify transformation by-products (TBPs).

329 The respective data are summarized in Table 2. A total number of 11 and 15 TBPs were
330 identified in the absence and presence of NaCl, respectively. According to these results,
331 polymerization pathways through radicals coupling were followed in the initial steps of
332 degradation both in the absence and presence of NaCl. The structures of BPA oligomers
333 (dimers, trimers and tetramers), as well as their formation pathways are depicted in Figure 8.
334 In general, for phenolic compounds, the formation of oligomers proceeds through C-C
335 coupling and/or C-O coupling. Among the two routes, C-C coupling (ortho-para and ortho-
336 ortho links) is a more favorable route, which is energetically promoted (Ežerskis and Jusys,
337 2001). However, it should be pointed out that TBPs with etheric structures have also been
338 identified previously via C-O coupling of phenoxy radicals and their formation can also be
339 expected (Ežerskis and Jusys, 2001).

340 Alongside the formation of dimers, trimers and tetramers, three other coupling TBPs (TBP2,
341 TBP4, TBP5) have been identified both in the absence and presence of NaCl. Their formation
342 pathways is depicted in Figure 9 and can be rationalized through the bimolecular coupling of
343 BPA radicals (I) and other radicals (e.g. V, VI, VII) originated from hydrogen abstraction and
344 β -scission of BPA and hydroxy-BPA.

345 Similar TBPs with oligomeric structures, as well as TBPs formed by coupling of different
346 radicals generated during the process have also been identified during the oxidation of BPA
347 by heat-activated persulfate (Potakis et al., 2017).

348 Besides the similarities in degradation pathways, some major differences are also pointed out.
349 In the presence of NaCl, chloro- and dichloro-BPA (TBP6 and TBP7) are formed at the first
350 stages of the reaction (Figure 10). Chlorine-substituted BPA derivatives have also been
351 reported in the literature during the chlorination of BPA molecule through a chlorine-
352 substitution reaction on the aromatic ring, followed by dehydration as the proposed
353 mechanism (Gallard et al., 2004; Hu et al., 2002). Based on literature data (Gallard et al.,

354 2004; Hu et al., 2002), 2-chloro-BPA, 2,6'-dichloro-BPA or 2,6-dichloro-BPA can be
355 postulated.

356 The rapid formation of chloro- and dichloro-BPA in combination with the high abundance of
357 their peaks justifies the fast kinetics of BPA degradation observed in the presence of NaCl.

358 The formation of TBP6 and TBP7 is followed by various chlorinated dimers and trimers, as a
359 result of coupling reactions depicted in Figure 10. However, in the absence of NaCl, the
360 degradation of BPA also proceeds through hydroxylation and oxidation reactions (Potakis et
361 al., 2017; Sharma et al., 2016) that can occur in the aromatic ring and isopropyl group (Figure
362 11). These pathways were not observed in the presence of NaCl within the same time
363 framework of treatment.

364 Although the concentration profiles of TBPs were not possible to be followed due to their fast
365 formation and dissipation, taking into account their relative abundance, it can be proposed
366 that radical coupling reactions are the main transformation pathways during the first stages of
367 the treatment, both in the presence and absence of NaCl. Comparing the polymerization
368 routes in the presence of NaCl, the formation of chlorinated dimers and trimers is
369 undoubtedly favored, proving the major role of chlorine radicals (Cl^\bullet) formed through the
370 direct reaction of Cl^- with $\text{SO}_4^{\bullet-}$ radicals, as also evidenced elsewhere (Lutze et al., 2015).

371

372 4. Conclusions

373 The primary conclusions derived from this study are as follows:

374 1) The rate of BPA degradation is a function of the operating variables, including catalyst,
375 oxidant and substrate concentrations, solution pH and treatment time. Similarly to other
376 Fenton-like AOPs, the rate increases with increasing catalyst and oxidant concentrations,
377 although excessive levels may introduce radical scavenging effects. Furthermore, the rate
378 decreases with increasing substrate concentration, which highlights the need to perform

379 studies with environmentally reasonable concentrations.

380 2) Unlike what typically happens in the advanced oxidation of various organics, BPA
381 degradation in environmentally relevant matrices is faster than in pure water; this pinpoints
382 the rather complicated interferences amongst the various organic and inorganic constituents
383 found in actual water matrices.

384 3) The individual effects of humic acid, alcohols, bicarbonate and chloride ions were
385 appraised; organics and the bicarbonate ion act as scavengers of sulfate and hydroxyl radicals,
386 thus leading to reduced degradation, while chlorides act as a source of extra Cl-containing
387 radicals, thus leading to increased degradation.

388 4) BPA degradation is accompanied by the formation of several TBPs and occurs through (i)
389 polymerization reactions, (ii) bimolecular coupling between BPA-radicals and other radicals,
390 and (iii) hydroxylation/oxidation reactions. Reactions in the presence of chlorides lead to the
391 formation of chlorinated TBPs.

392

393 Acknowledgments

394 Z. Frontistis would like to thank the Greek State Scholarships Foundation (IKY) for the
395 financial support of this research through the “IKY Fellowships of Excellence for
396 Postgraduate Studies in Greece – Siemens Programme” in the framework of the Hellenic
397 Republic – Siemens Settlement Agreement.

398 Part of this work was financially supported by: Project POCI-01-0145-FEDER-006984 -
399 Associate Laboratory LSRE-LCM funded by FEDER through COMPETE2020 – Programa
400 Operacional Competitividade e Internacionalização (POCI) - and by national funds through
401 FCT - Fundação para a Ciência e a Tecnologia. R.S. Ribeiro acknowledges the FCT
402 individual Ph.D. grant SFRH/BD/94177/2013, with financing from FCT and the European
403 Social Fund (through POPH and QREN). A.M.T. Silva acknowledges the FCT Investigator
404 2013 Programme (IF/01501/2013), with financing from the European Social Fund and the

405 Human Potential Operational Programme.

406

407 References

408

409 Anipsitakis, G.P., Dionysiou, D.D., Gonzalez, M.A., 2006. Cobalt-mediated activation of
410 peroxymonosulfate and sulfate radical attack on phenolic compounds. Implications of
411 chloride ions. *Environmental Science & Technology* 40 (3), 1000-1007.

412 Bautista-Toledo, I., Ferro-Garcia, M.A., Moreno-Castilla, C., Vegas Fernandez, F.J., 2005.
413 Bisphenol A removal from water by activated carbon. Effects of carbon characteristics and
414 solution chemistry. *Environmental Science & Technology* 39 (16), 6246-6250.

415 Bennedsen, L.R., Muff, J. Sogaard, E.G., 2012. Influence of chloride and carbonates on the
416 reactivity of activated persulfate. *Chemosphere* 86 (11), 1092-1097.

417 Darsinou, B., Frontistis, Z., Antonopoulou, M., Konstantinou, I., Mantzavinos, D., 2015.
418 Sono-activated persulfate oxidation of bisphenol A: Kinetics, pathways and the controversial
419 role of temperature. *Chemical Engineering Journal* 280, 623-633.

420 Dewil, R., Mantzavinos, D., Poulios, I., Rodrigo, M.A., 2017. New perspectives for advanced
421 oxidation processes. *Journal of Environmental Management* 195, 93-99.

422 Ežerskis, Z., Jusys, J., 2001. Electropolymerization of chlorinated phenols on a Pt electrode in
423 alkaline solution Part I: A cyclic voltammetry study. *Journal of Applied Electrochemistry*, 31
424 (10) 1117-1124.

425 Fang, G.D., Dionysiou, D.D., Wang, Y., Al-Abed, S.R., Zhou, D.M., 2012. Sulfate radical-
426 based degradation of polychlorinated biphenyls: Effects of chloride ion and reaction kinetics.
427 *Journal of Hazardous Materials* 227-228, 394-401.

428 Gallard, H., Leclercq, A., Croué, J.P., 2004. Chlorination of bisphenol A: kinetics and by-
429 products formation. *Chemosphere* 56 (5), 465-473.

430 Hu, J.Y., Aizawa, T., Ookubo, S., 2002. Products of aqueous chlorination of BPA and the
431 estrogenic activity. *Environmental Science & Technology* 36 (9), 1980-1987.

432 Huang, Y.Q., Wong, C.K.C., Zheng, J.S., Bouwman, H., Barra, R., Wahlstrom, B., Neretin,
433 L., Wong, M.H., 2012. Bisphenol A (BPA) in China: a review of sources, environmental
434 levels, and potential human health impacts. *Environment International* 42, 91-99.

435 Lin, Y.T., Liang, C., Chen, J.H., 2011. Feasibility study of ultraviolet activated persulfate
436 oxidation of phenol. *Chemosphere* 82 (8), 1168-1172.

437 Liu, H., Bruton, T.A., Doyle, F.M., Sedlak, D.L., 2014. In situ chemical oxidation of
438 contaminated groundwater by persulfate: Decomposition by Fe(III)- and Mn(IV)-containing
439 oxides and aquifer materials. *Environmental Science & Technology* 48 (17), 10330-10336.

440 Lutze, H.V., Kerlin, N., Schmidt, T.C., 2015. Sulfate radical-based water treatment in
441 presence of chloride: Formation of chlorate, inter-conversion of sulfate radicals into hydroxyl
442 radicals and influence of bicarbonate. *Water Research* 72, 349-360.

443 Matzek, L.W., Carter, K.E., 2016. Activated persulfate for organic chemical degradation: A
444 review. *Chemosphere* 151, 178-188.

445 Nidheesh, P.V., 2015. Heterogeneous Fenton catalysts for the abatement of organic pollutants
446 from aqueous solution: a review. *RSC Advances* 5, 40552-40577.

447 Oehlmann, J., Oetken, M., Schulte-Oehlmann, U., 2008. A critical evaluation of the
448 environmental risk assessment for plasticizers in the freshwater environment in Europe, with
449 special emphasis on bisphenol A and endocrine disruption. *Environmental Research* 108 (2),
450 140-149.

451 Potakis, N., Frontistis, Z., Antonopoulou, M., Konstantinou, I., Mantzavinos, D., 2017.
452 Oxidation of bisphenol A in water by heat-activated persulfate. *Journal of Environmental*
453 *Management* 195, 125-132.

454 Qi, C., Liu, X., Zhao, W., Lin, C., Ma, J., Shi, W., Sun, Q., Xiao, H., 2015. Degradation and
455 dechlorination of pentachlorophenol by microwave-activated persulfate. *Environmental*
456 *Science & Pollution Research* 22 (6), 4670-4679.

457 Ribeiro, R.S., Silva, A.M.T., Figueiredo, J.L., Faria, J.L., Gomes, H.T., 2016a. Catalytic wet
458 peroxide oxidation: a route towards the application of hybrid magnetic carbon
459 nanocomposites for the degradation of organic pollutants. A review. Applied Catalysis B -
460 Environmental 187, 428-460.

461 Ribeiro, R.S., Frontistis, Z., Mantzavinos, D., Venieri, D., Antonopoulou, M., Konstantinou,
462 I., Silva, A.M.T., Faria, J.L., Gomes, H.T., 2016b. Magnetic carbon xerogels for the catalytic
463 wet peroxide oxidation of sulfamethoxazole in environmentally relevant water matrices.
464 Applied Catalysis B - Environmental 199, 170-186.

465 Sharma, J., Mishra, I.M., Kumar, V., 2016. Mechanistic study of photo-oxidation of bisphenol
466 A (BPA) with hydrogen peroxide (H₂O₂) and sodium persulfate (SPS). Journal of
467 Environmental Management 166, 12-22.

468 Tsitonaki, A., Petri, B., Crimi, M., Mosbaek, H., Siegrist, R.L., Bjerg, P.L., 2010. In situ
469 chemical oxidation of contaminated soil and groundwater using persulfate: A review. Critical
470 Reviews in Environmental Science & Technology 40 (1), 55-91.

471 Vandenberg, L.N., Hauser, R., Marcus, M., Olea, N., Welshons, W.V., 2007. Human
472 exposure to bisphenol A (BPA). Reproductive Toxicology 24 (2), 139-177.

473 Vicente, F., Santos, A., Romero, A., Rodriguez, S., 2011. Kinetic study of diuron oxidation
474 and mineralization by persulphate: effects of temperature, oxidant concentration and iron
475 dosage method. Chemical Engineering Journal 170 (1), 127-135.

476 Zhao, L., Hou, H., Fujii, A., Hosomi, M., Li, F., 2014. Degradation of 1,4-dioxane in water
477 with heat- and Fe²⁺-activated persulfate oxidation. Environmental Science & Pollution
478 Research 21 (12), 7457-7465.

479 **Table 1.** Properties of the water matrices used in this work. ND: not determined.

Property	UPW	Wastewater	Drinking water	Surface water	Groundwater
pH	6	8	7.5	7.5	7.4
Conductivity, $\mu\text{S/cm}$	0.056	311	396	491	798
TOC, mg/L		7		2.7	1.9
Bicarbonate, mg/L		182	211	ND	ND
Chloride, mg/L		0.5	9.8	5	76
Sulfate, mg/L		30	15	274	69.5
Nitrate, mg/L		57	5		18.8

480

481 **Table 2.** High resolution accurate mass data ($[M-H]^-$, and relative error $\Delta(\text{ppm})$) for BPA and
 482 TBPs (a) in the absence of NaCl, and (b) in the presence of NaCl.
 483

TBP code	Ion elemental composition	m/z $[M-H]^-$	Δ (ppm)	Process
BPA	$C_{15}H_{15}O_2$	227.1074	1.6	
TBP1	$C_{15}H_{13}O_4$	257.0821	-0.6	a
TBP2	$C_{18}H_{21}O_4$	301.1443	0.9	a
TBP3	$C_{15}H_{13}O_3$	241.0876	-2.4	a,b
TBP4	$C_{15}H_{15}O_3$	243.1028	-0.3	a,b
TBP5	$C_{24}H_{25}O_4$	377.1744	3.7	a,b
TBP6	$C_{15}H_{14}ClO_2$	261.0675	4.8	b
TBP7	$C_{15}H_{13}Cl_2O_2$	295.0297	0.4	b
TBP8	$C_{30}H_{29}O_4$	453.2059	2.8	a,b
TBP9	$C_{60}H_{57}O_8$	905.4019	4.4	a,b
TBP10	$C_{30}H_{28}ClO_4$	487.1682	-0.1	b
TBP11	$C_{30}H_{29}O_4$	453.2057	3.9	a,b
TBP12	$C_{30}H_{27}Cl_2O_4$	521.1280	2.4	b
TBP13	$C_{45}H_{43}O_6$	679.3059	0.8	a,b
TBP14	$C_{45}H_{42}ClO_6$	713.2649	3.7	b
TBP15	$C_{45}H_{43}O_6$	679.3041	3.6	a,b
TBP16	$C_{45}H_{43}O_6$	679.3065	0	a,b
TBP17	$C_{45}H_{42}ClO_6$	713.2675	0.1	b

484

485 Figure captions

486

487 **Figure 1.** Effect of buffered solution pH on 285 µg/L BPA degradation with 75 mg/L
488 CX/CoFe and 250 mg/L SPS in UPW.

489 **Figure 2.** Effect of CX/CoFe concentration on 285 µg/L BPA degradation with 250 mg/L
490 SPS in UPW and pH=3.

491 **Figure 3.** Effect of SPS concentration on 285 µg/L BPA degradation with 75 mg/L CX/CoFe
492 in UPW and pH=3. Dashed line shows experiment with 250 mg/L hydrogen peroxide (HP) in
493 otherwise identical conditions.

494 **Figure 4.** Effect of initial BPA concentration on its degradation with 75 mg/L CX/CoFe and
495 250 mg/L SPS in UPW and pH=3.

496 **Figure 5.** Effect of actual water matrix on 285 µg/L BPA degradation with 75 mg/L
497 CX/CoFe, 250 mg/L SPS and pH=3.

498 **Figure 6.** Effect of organics on 285 µg/L BPA degradation with 75 mg/L CX/CoFe and 250
499 mg/L SPS in UPW and pH=3.

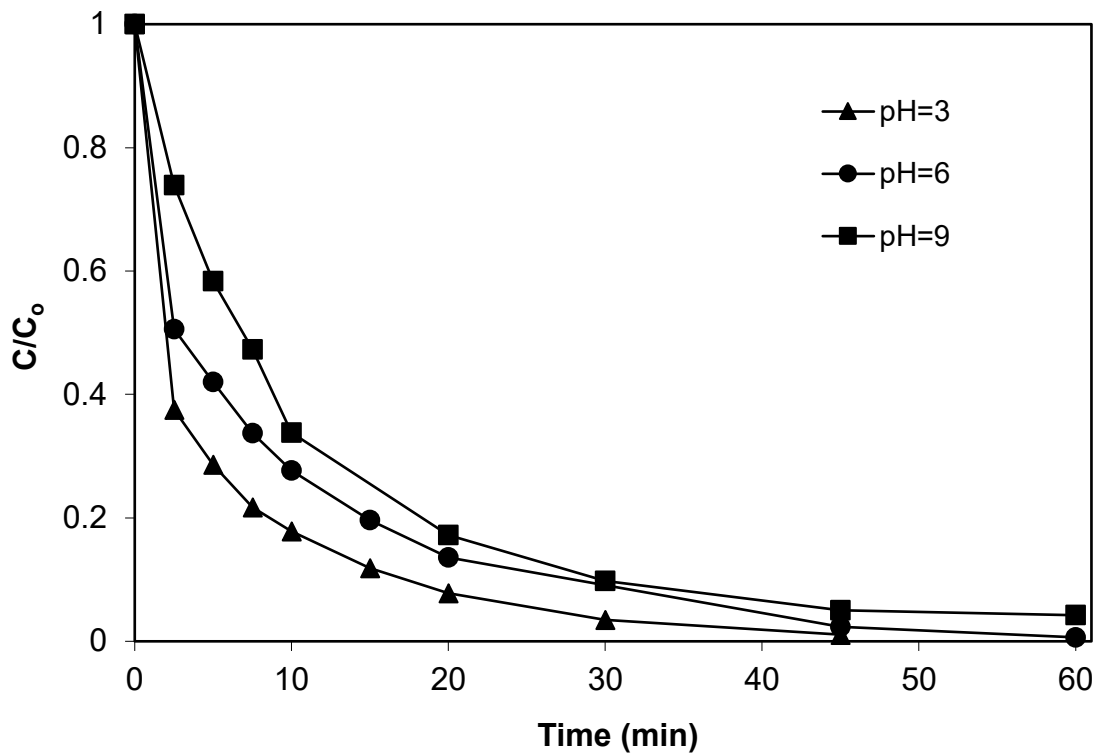
500 **Figure 7.** Effect of NaCl on 285 µg/L BPA degradation with 75 mg/L CX/CoFe and 250
501 mg/L SPS in UPW and pH=3.

502 **Figure 8.** BPA transformation pathways by BPA-radical coupling during treatment with
503 CX/CoFe and SPS in the presence and absence of NaCl.

504 **Figure 9.** BPA transformation pathways by radical coupling after β-scission of BPA-radical
505 during treatment with CX/CoFe and SPS in the presence and absence of NaCl.

506 **Figure 10.** BPA transformation pathways during treatment with CX/CoFe and SPS in the
507 presence of NaCl.

508 **Figure 11.** Hydroxylation degradation pathways of BPA during treatment with CX/CoFe and
509 SPS in the absence of NaCl.

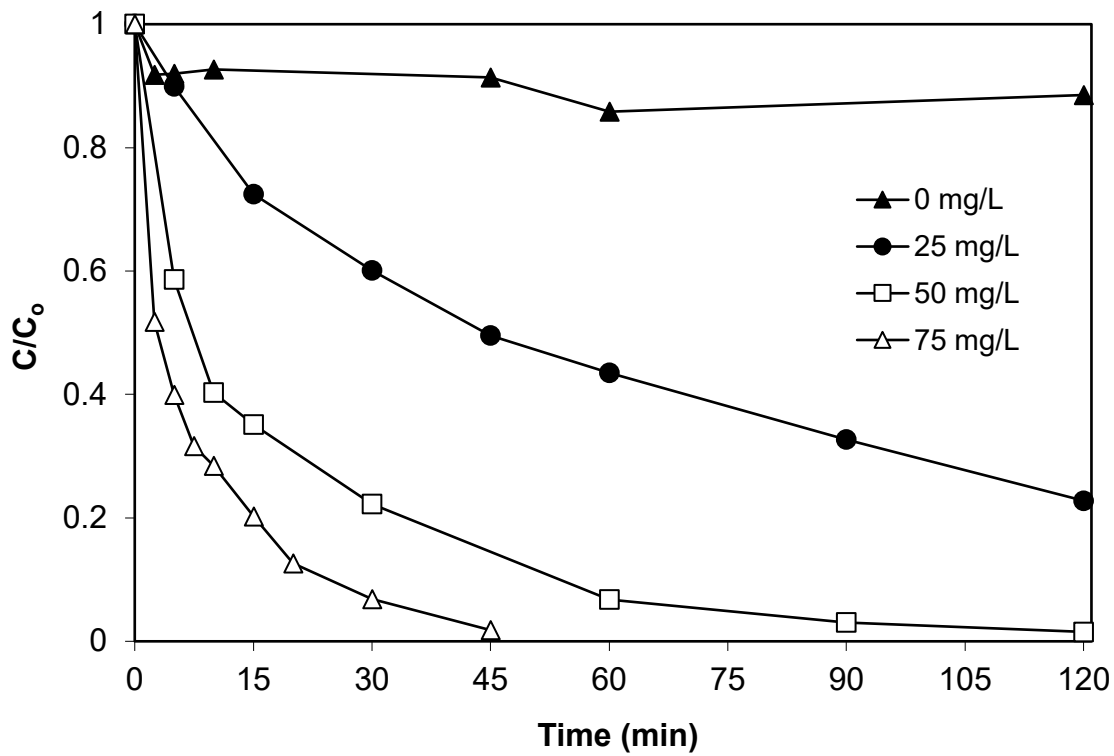


510

511

512 **Figure 1.** Effect of buffered solution pH on 285 $\mu\text{g/L}$ BPA degradation with 75 mg/L
513 CX/CoFe and 250 mg/L SPS in UPW.

514



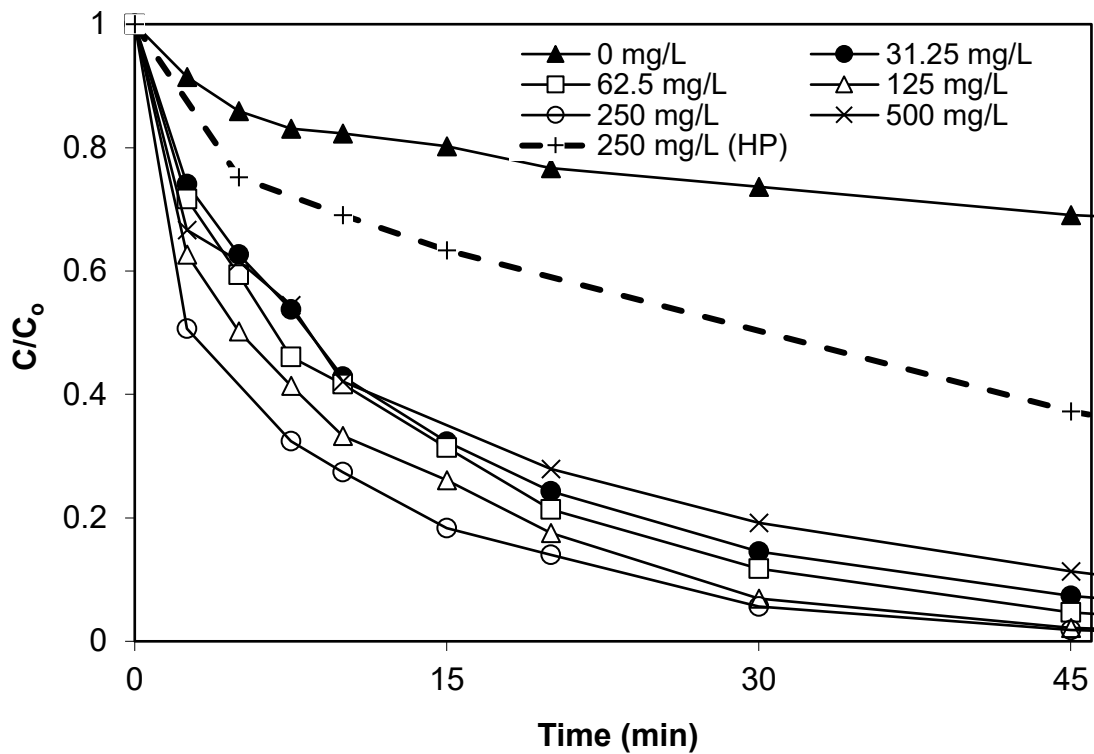
515

516

517 **Figure 2.** Effect of CX/CoFe concentration on 285 µg/L BPA degradation with 250 mg/L

518 SPS in UPW and pH=3.

519

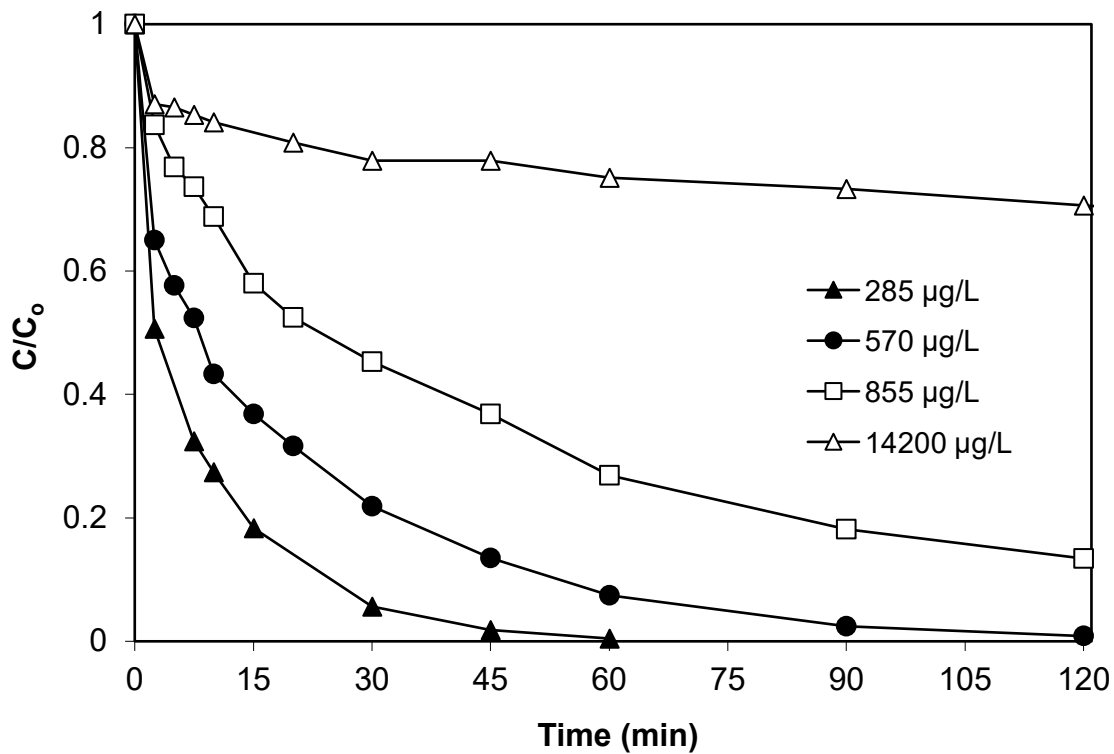


520

521

522 **Figure 3.** Effect of SPS concentration on 285 $\mu\text{g/L}$ BPA degradation with 75 mg/L CX/CoFe
 523 in UPW and pH=3. Dashed line shows experiment with 250 mg/L hydrogen peroxide (HP) in
 524 otherwise identical conditions.

525

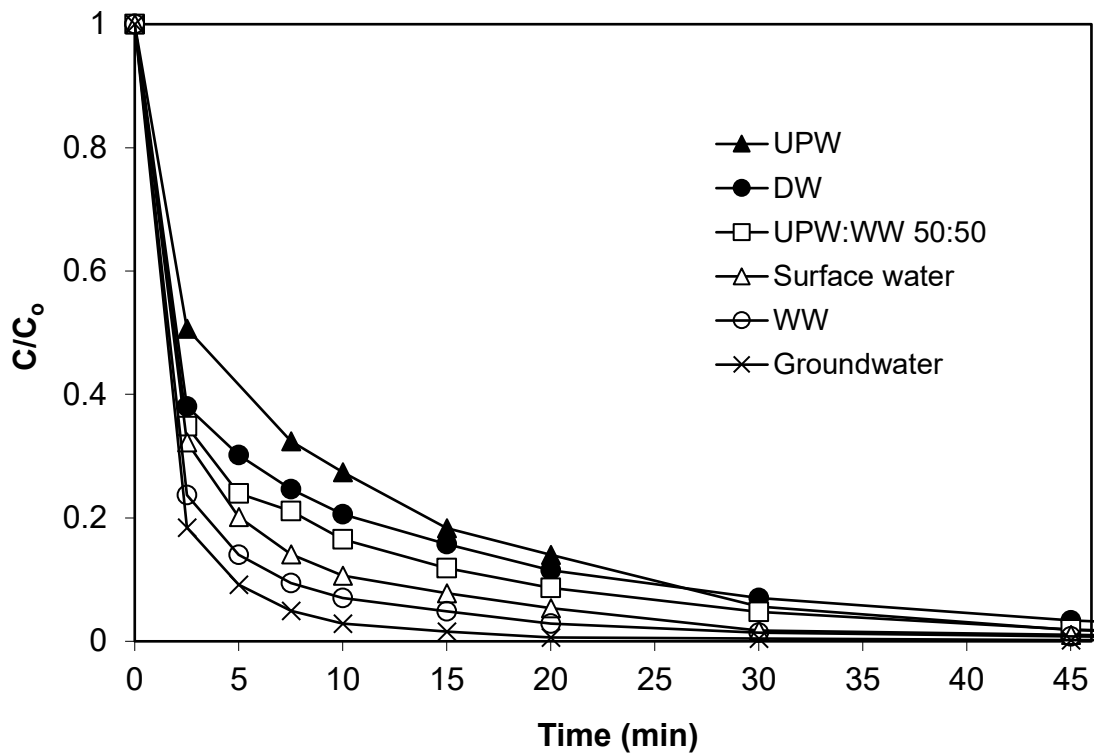


526

527

528 **Figure 4.** Effect of initial BPA concentration on its degradation with 75 mg/L CX/CoFe and
 529 250 mg/L SPS in UPW and pH=3.

530



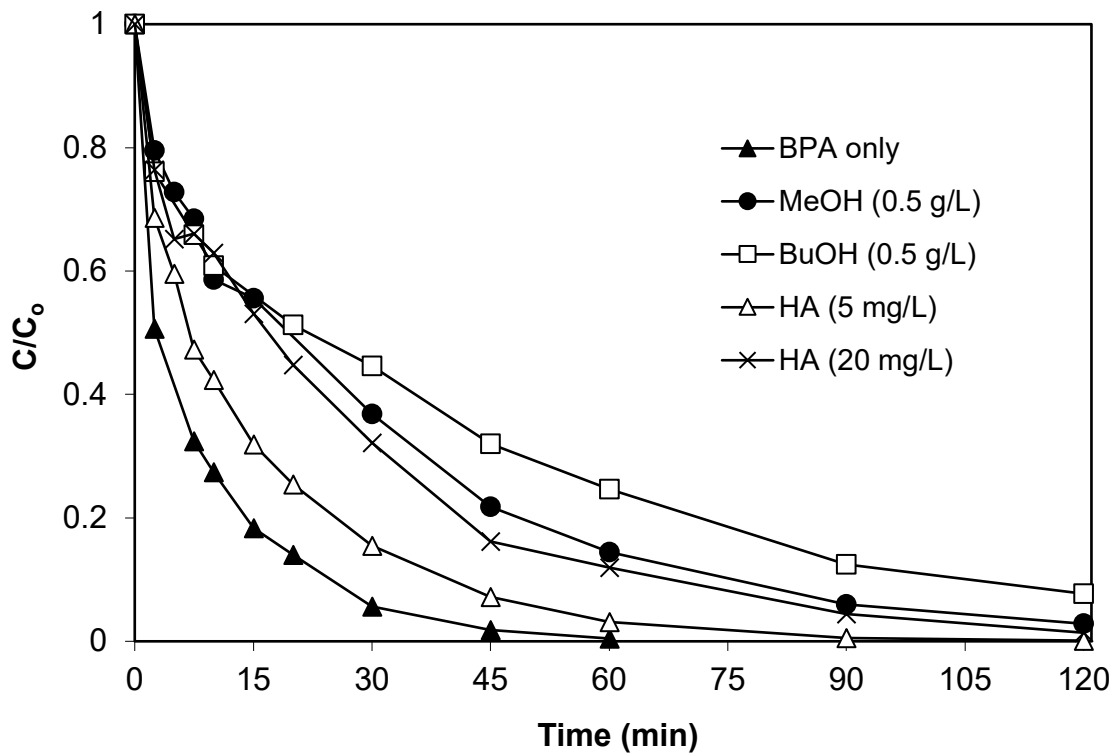
531

532

533 **Figure 5.** Effect of actual water matrix on 285 $\mu\text{g/L}$ BPA degradation with 75 mg/L

534 CX/CoFe, 250 mg/L SPS and pH=3.

535

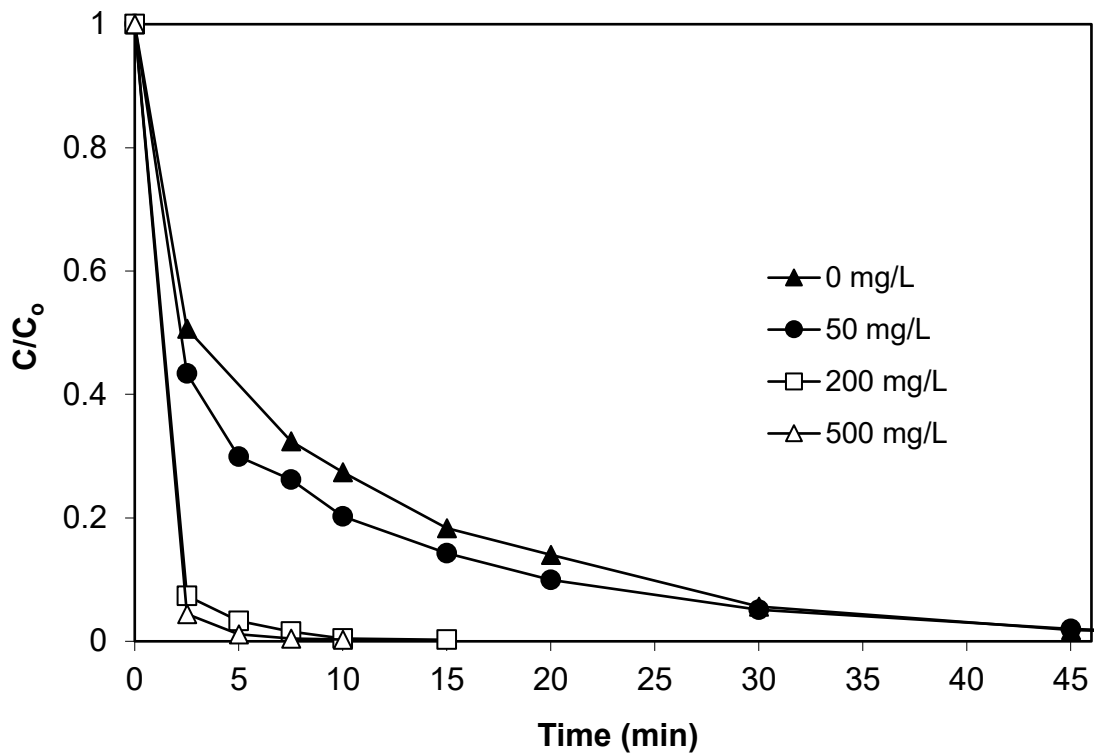


536

537

538 **Figure 6.** Effect of organics on 285 $\mu\text{g/L}$ BPA degradation with 75 mg/L CX/CoFe and 250
 539 mg/L SPS in UPW and pH=3.

540

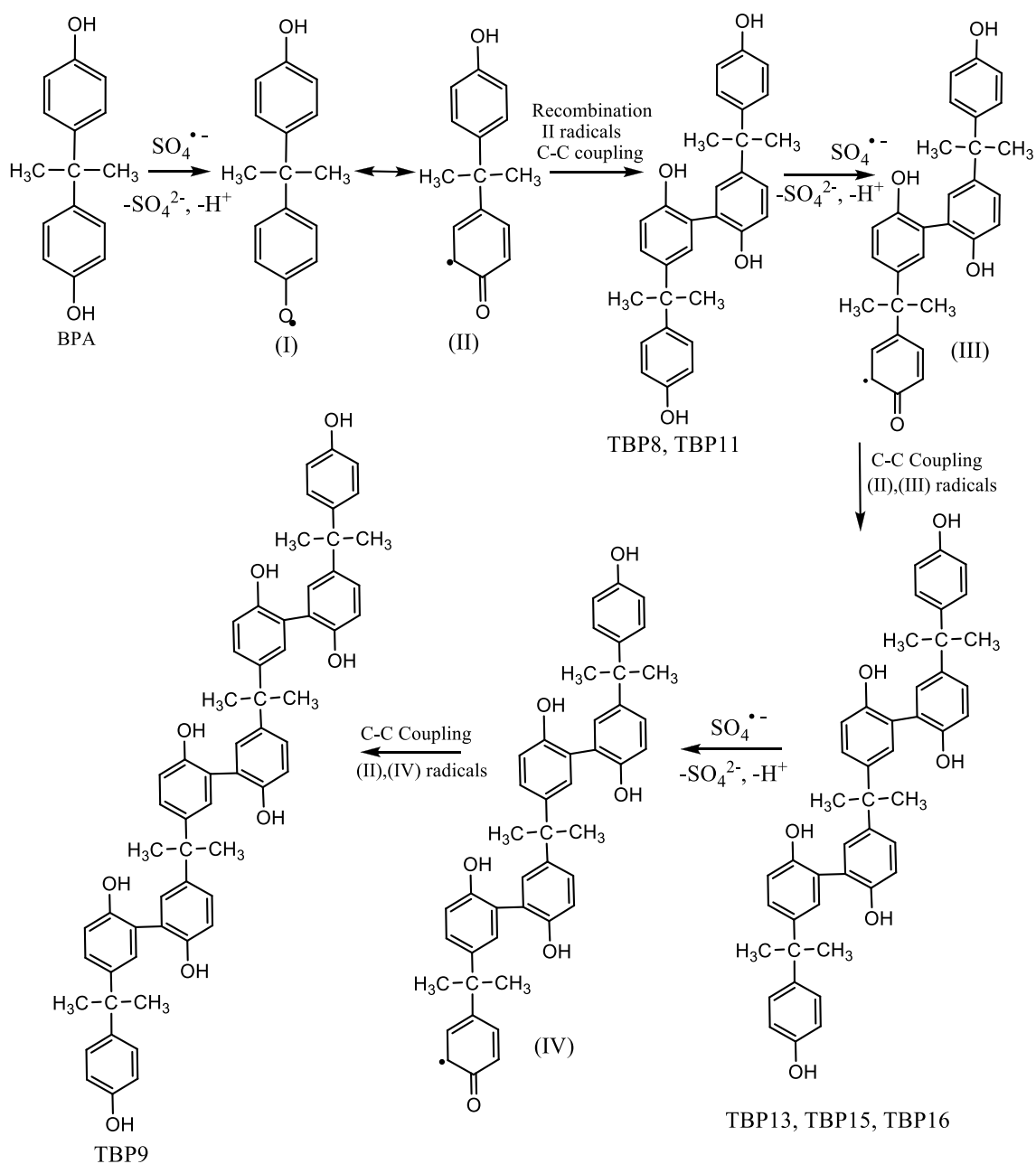


541

542

543 **Figure 7.** Effect of NaCl on 285 $\mu\text{g/L}$ BPA degradation with 75 mg/L CX/CoFe and 250
 544 mg/L SPS in UPW and pH=3.

545

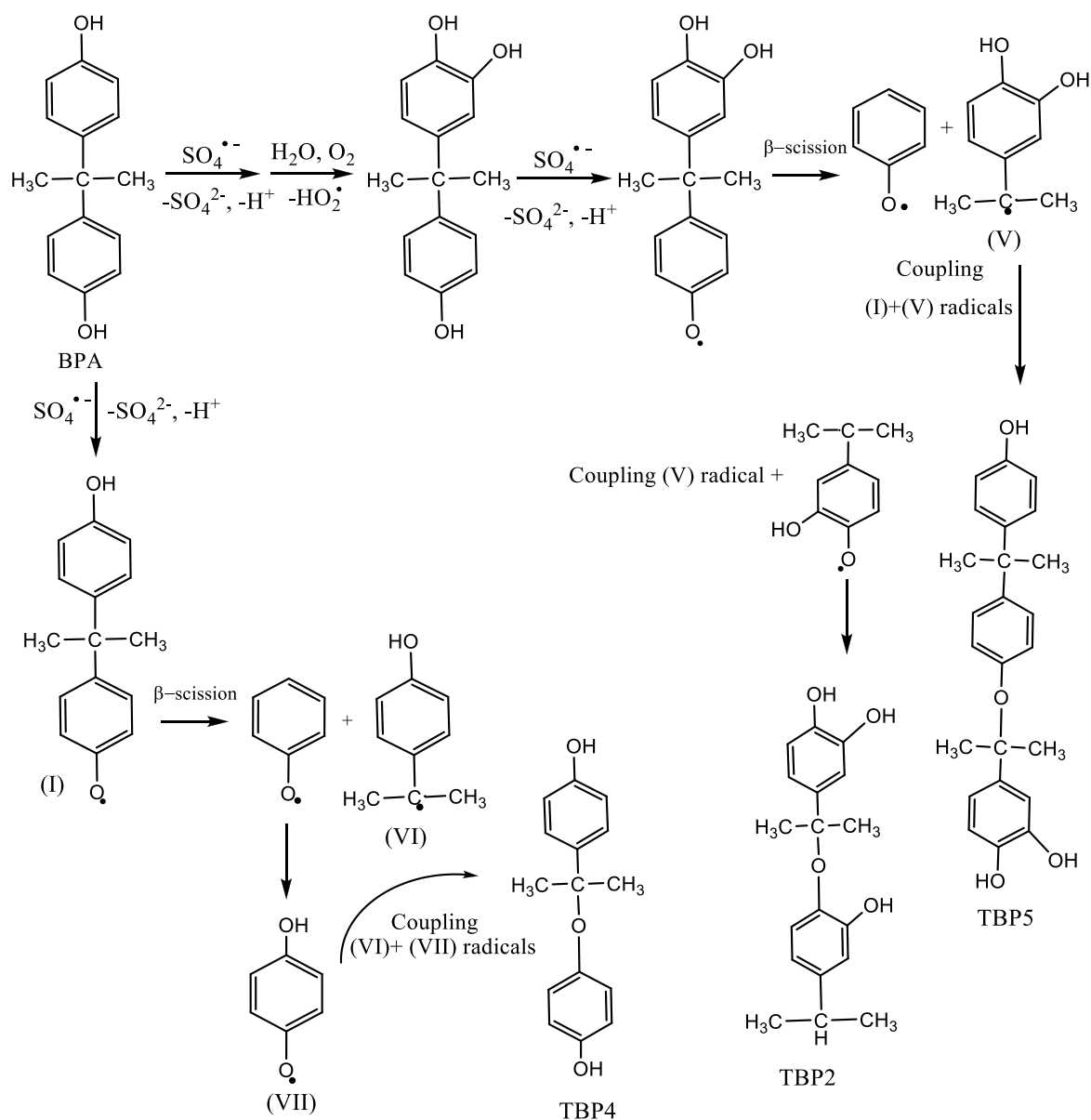


546

547

548 **Figure 8.** BPA transformation pathways by BPA-radical coupling during treatment with

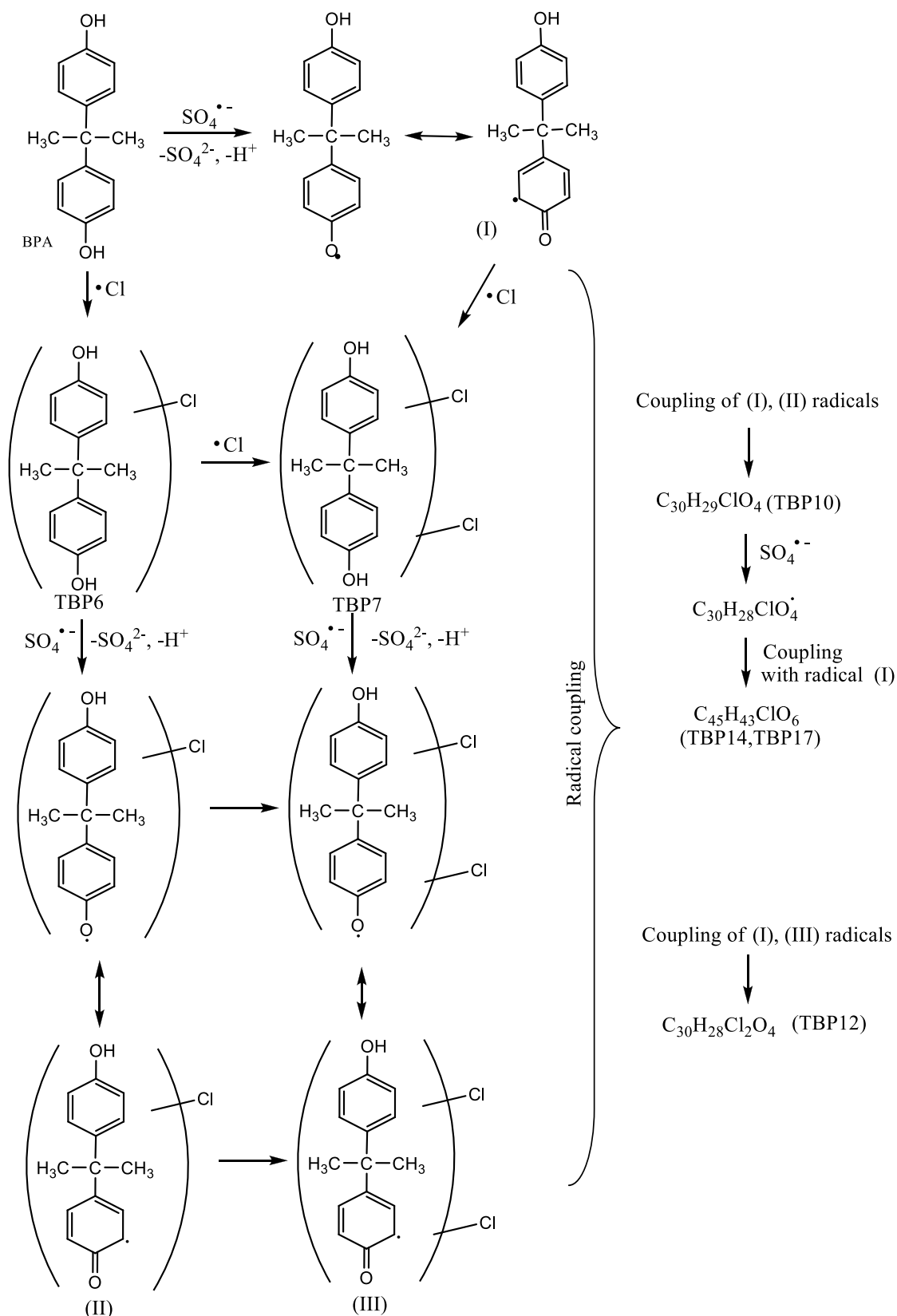
549 CX/CoFe and SPS in the presence and absence of NaCl.



550

551 **Figure 9.** BPA transformation pathways by radical coupling after β -scission of BPA-radical

552 during treatment with CX/CoFe and SPS in the presence and absence of NaCl.



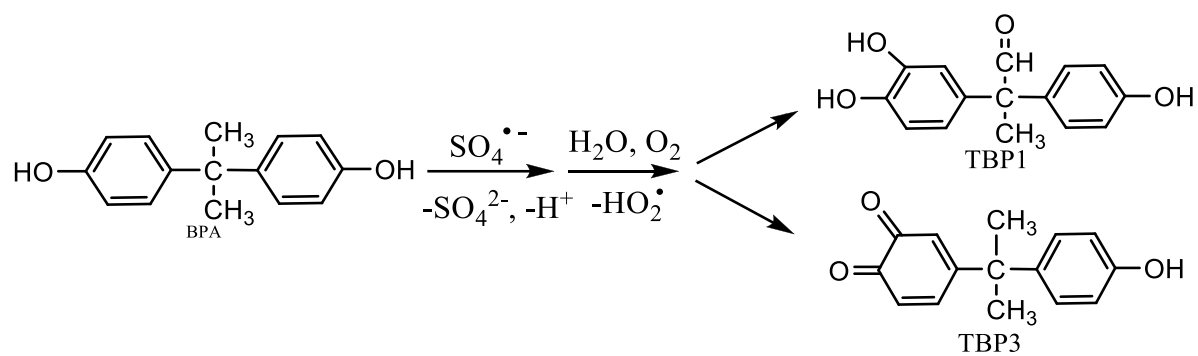
553

554

555 **Figure 10.** BPA transformation pathways during treatment with CX/CoFe and SPS in the
 556 presence of NaCl.

557

558



559

560

561 **Figure 11.** Hydroxylation degradation pathways of BPA during treatment with CX/CoFe and

562 SPS in the absence of NaCl.